RSC Advances

ROYAL SOCIETY OF CHEMISTRY

www.rsc.org/advances

RSC Advances

ARTICLE

Degradation of organic pollutants by $NiFe_2O_4$/peroxymonosulfate: Efficiency, influential factors and catalytic mechanism†

Received 00th January 20xx,
Accepted 00th January 20xx

DOI: 10.1039/x0xx00000x

www.rsc.org/

Zilin Wang,[a] Yunchen Du,*[ab] Yulei Liu,[a] Bohua Zou,[b] Jiayue Xiao,[a] and Jun Ma*[a]

Nickel ferrites ($NiFe_2O_4$) were prepared through thermal decomposition of homogeneous nickel oxalate and ferrous oxalate, and the product displayed typical spinel structure, small nanoparticle size (*ca.* 12 nm), high BET surface (53.5 m^2/g), and good magnetic response (19.3 emu/g). The as-prepared $NiFe_2O_4$ was applied in heterogeneous catalysis to generate powerful radicals from peroxymonosulfate (PMS) for the removal of recalcitrant pollutant. Herein, benzoic acid (BA) was employed as a stable model organic pollutant, and it was found that $NiFe_2O_4$/PMS system could realize 82.5% degradation in 60 min and maintain its catalytic efficiency during four recycling experiments. Such a catalytic performance of $NiFe_2O_4$ was indeed superior to those from Fe_2O_3 (23.5%), Fe_3O_4 (48.0%), NiO (57.6%), and $MnFe_2O_4$ (63.8%). Although $NiFe_2O_4$ performed a slightly inferior BA degradation to $CoFe_2O_4$ (86.2%), its nickel leaching (0.265 mg/L) was much less than cobalt leaching (0.384 mg/L) from $CoFe_2O_4$. In addition, some potential influential factors, including the dosages of PMS and $NiFe_2O_4$, the initial pH value, ion strength, and the concentrations of bicarbonate, natural organic matter, halide, were systemically investigated. More importantly, $NiFe_2O_4$/PMS were also effective for BA removal under some actual water background conditions, especially in surface water and the finished water from drinking water treatment plant: the degradation efficiencies of BA were still close up to 60%. Sulfate and hydroxyl radicals were confirmed to be the main reactive species in the $NiFe_2O_4$/PMS system. XPS spectra revealed that Ni sites on the surface of $NiFe_2O_4$ were the primary active sites, and Raman spectra suggested that inner-sphere complexation between PMS and Ni sites derived peroxo species on the surface, which were further responsible for the efficient generation of radicals.

Introduction

Dissolved organic pollutants, which are perennially challenging for conventional water treatment processes, can be efficiently removed by advanced oxidation technologies (AOTs). Hydroxyl radicals (·OH), were widely studied as characteristic species in AOTs because of their notable reactivity towards organic compounds. However, hydroxyl radicals, no matter how they were generated (e.g. ozone, Fenton/Fenton-like process), suffered from many limitations in application, such as sophisticated and cost-intensive radical generation processes, pH adjustments and potential sludge generation.[1-3]

In the past decade, increasing research interests were attracted by sulfate-radical based advanced oxidation technologies (SR-AOTs) in which sulfate radicals ($SO_4^{\bullet-}$) were the main reactive species, because they could perform better than conventional hydroxyl radicals due to their higher reduction potential (2.5~3.1 V).[4, 5] $SO_4^{\bullet-}$ was generally released from peroxymonosulfate (PMS) or peroxydisulfate (PDS) by heating, UV irradiation or ultrasound.[6-8] The high-energy input meant that these techniques could hardly be applied extensively because of their cost-ineffectiveness. Recent research progress suggested that some transition metal ions, such as Ni^{2+}, Fe^{3+}, and Co^{2+}, were highly effective for persulfate activation in homogeneous system, where the released radicals could lead to the degradation of organic pollutants.[9] However, the toxicity caused by the overload of transition metal ions severely hindered the application of this method in water treatment.[9] Therefore, it is significant to develop new persulfate activators, which could be characterized by not only remarkable and stable catalytic activity with decreasing metal leaching, but also being easily separated from water.[10]

Spinel ferrites, with the general formula MFe_2O_4 (M= Fe, Cu, Co, Ni, etc.), are receiving more and more attention due to their good activity, stable structure, extremely low solubility, and easily magnetic separation.[11-18] For example, Deng et al. reported that $CoFe_2O_4$ nanoparticles could be used for the activation of PMS to generate sulfate radicals for the degradation of diclofenac, and the high catalytic activity and good catalytic stability could be retained for several successive cycles;[12] Zhang et al. found that the production of radical species from PMS induced by a magnetic $CuFe_2O_4$ spinel was a simple, nonhazardous, efficient and low energy-consuming process, and $CuFe_2O_4$ showed higher activity and 30 times lower Cu^{2+} leaching than a well-crystallized CuO at the same dosage;[14] Yao et al. also demonstrated the excellent Fenton-

[a] *State Key Laboratory of Urban Water Resource and Environment, School of Municipal and Environmental Engineering, Harbin Institute of Technology, Harbin 150001, China.*
Email: majun@hit.edu.cn (J. Ma); yunchendu@hit.edu.cn (Y.C. Du).
[b] *Department of Chemistry, Harbin Institute of Technology, Harbin 150001, China.*

† Electronic Supplementary Information (ESI) available: HR-TEM image; capacity of mineralization; EEM images for different reaction time; the effect of NiO dosage; EEM images and components of actual water bodies; the inhibition of phosphate; XPS spectra of fresh and used $NiFe_2O_4$. See DOI: 10.1039/x0xx00000x

like activities and magnetic property for easy separation of $MnFe_2O_4$ nanoparticles, as well as their good durability on the elimination of organic dyes by PMS oxidation.[15] All results indicated that the activation of PMS by spinel ferrites will be a green oxidation process with promising potentials in the application of contamination control.

As a typical member of spinel ferrites, $NiFe_2O_4$ has displayed its good ability in activating ozone molecular to release hydroxyl radicals for the degradation of organic pollutants,[19, 20] and it could even afford much better removal efficiency of organic pollutants than conventional homogeneous photocatalysis and biodegradation techniques.[19] Therefore, the activity of $NiFe_2O_4$ for PMS activation can be expected, while it is unfortunate that few papers presented a systematic study on the performance of $NiFe_2O_4$ to date. In addition, most experiments on the aforementioned spinel ferrites were performed in the system of high-purity water, and the real catalytic behaviors under some actual water backgrounds were rarely mentioned. In this paper, we synthesized magnetic nickel ferrite by thermal decomposition of transition metal oxalate, and investigated its catalysis activity towards sulfate radical generation for the first time. Benzoic acid (BA) was selected as a stable model organic pollutant in this system since it can easily react with radicals, but it is hardly degraded via non-radical process.[21] The properties of $NiFe_2O_4$ were characterized, and the catalytic performance was examined by comparing with other metal oxides and spinel ferrites. Potential influential factors were fully explored, as well as the mechanisms of radical generation. More importantly, the as-prepared $NiFe_2O_4$ was also applied to the treatment of organics under some actual water background conditions.

Experimental section

Chemical reagents

Oxone ($KHSO_5 \cdot 0.5KHSO_4 \cdot 0.5K_2SO_4$, PMS), benzoic acid (BA, 99.5%) and humic acid (HA) were of ACS reagent grade and purchased from Sigma-Aldrich. Nickel nitrate, ferrous sulfate and ammonium oxalate used for spinel synthesis were all of analytical-reagent grade and purchased from Tianjin Chemical Reagent Co., Ltd. Nickel(II) oxide, iron(II) oxide, iron(II,III) oxide, sodium hydroxide, perchloric acid, sodium bicarbonate, potassium chloride, potassium bromide and sodium perchlorate used in the catalysis were all of analytical-reagent grade and purchased from Sinopharm Chemical Reagent Co., Ltd. Methanol (MeOH) purchased from TEDIA and acetic acid purchased from Dikama were both of HPLC grade. *Tert*-butyl-alcohol (TBA) was of guaranteed reagent grade and supplied by Sinopharm Chemical Reagent Co., Ltd. All solutions were used without any further purification, and prepared with ultrapure water produced by a Milli-Q Biocel water system.

Materials synthesis and characterization

The $NiFe_2O_4$ was prepared by thermal decomposition of mixed inorganic salts.[22] Briefly, 11.65 g of $FeSO_4 \cdot 7H_2O$ and 4.53 g of $NiCl_2 \cdot 6H_2O$ were dissolved in 40 mL Milli-Q water. The stoichiometric ratio of Fe(II) and Ni(II) was 2.2:1 with slight overweight of Fe(II) to suppress the formation of NiO phase. This solution was poured into 200 mL saturated $(NH_4)_2C_2O_4$ solution, and stirred for 30 min. After that, the precipitation was collected by filtration and then calcined at 400°C for 4 h.

The surface morphology of $NiFe_2O_4$ spinel was obtained by using a Quanta 200S (Fei, USA) scanning electronic microscopy (SEM). Transmission electron microscope (TEM) image was obtained on a Tecnai G^2 F30 operating at an accelerating voltage of 200 kV. Powder X-ray diffraction (XRD) data were recorded on a Rigaku D/MAXRC X-ray diffractometer with Cu Kα radiation source (45.0 kV, 50.0 mA). Nitrogen adsorption isotherms were obtained at 196 °C on a QUADRASORB SI-KR/MP (Quantachrome, USA). Samples were normally prepared for measurement by degassing at 120 °C. Pore size distributions were calculated using Barrett-Joyner-Halenda (BJH) method. The magnetic hysteresis loops of $NiFe_2O_4$ were made with a LakeShore 7404 (LakeShore, USA) vibrating sample magnetometer (VSM). X-ray photoelectron spectroscopy (XPS) analysis was performed on PHI 5700 ESCA System (Physic Electronics, USA) with an Al Kα 1486.6 eV radiation sources. The pH_{pzc} of the spinel was obtained by mass titration according to previous literature.[23] In situ Raman analysis of $NiFe_2O_4$ surface in the presence and absence of PMS was carried out on a confocal microscopic Raman spectrometer (Renishaw, In Via) equipped with a 633 nm laser light irradiation. $NiFe_2O_4$ powder or $NiFe_2O_4$/PMS powder (mass ratio at 5:1) was mixed and pressed into slices of about 1 mm in thickness. Milli-Q water was dropped onto the slice, and then Raman spectra were taken on the surface of $NiFe_2O_4$ particle by a quick scan from 800 to 1100 cm^{-1} with a laser power of 15 mW. The irradiation did not cause PMS decomposition in the solution.

Experimental procedure and analysis

All the catalytic experiments were performed in 200 mL conical flask at 25±1°C, where the rotary speed was 100 rpm. Certain amounts of PMS and BA solution were added into the flask to a total volume of 100 mL without any buffer. The initial pH value of the solution was adjusted by NaOH/$HClO_4$. The oxidative process was initiated when the catalyst was introduced. After withdrawing from the flasks, samples were filtered by a glass fiber membrane (φ: 0.22 μm), and quenched by excessive sodium thiosulfate. For the recycling test of $NiFe_2O_4$, several identical reactions were performed simultaneously. The used catalysts were separated by filtration and evaporated at 80 °C for re-usage.

Several water bodies were employed as actual water backgrounds. Raw water (I-DWTP) and the finished water (FW-DWTP) from a drinking water treatment plant in Heilongjiang Province, China, were applied for comparing the degradation efficiencies by pre-/post-oxidation. Surface water from Songhua River in Harbin, China, the effluent from a biological reactor with domestic waste water as influent (E-WWTP), and groundwater from Harbin were also used for investigating the influence of background substances.

The concentration of BA was quantified by a Waters 2695 high performance liquid chromatography (HPLC) with Waters 2998 photodiode array detector (Waters, USA) at λ=263 nm. The eluent of water (0.5‰ acetic acid) and methanol was in the ratio of 50:50 at a flow rate of 1.0 mL/min. Leaching nickel ions were measured with an Optima 8300 (PerkinElmer, USA) ICP-OES. The concentration of halide ions were determined by an ICS-3000 (Dionex, USA) ion chromatograph. The concentrations of total carbon, inorganic carbon and total organic carbon were confirmed by a Multi N/C 3100 (Jena, Germany) TOC analyzer. Excitation emission matrix (EEM) fluorescence spectra were obtained by an F-70000 (HITACH, Japan) fluorescence spectrometer.

Results and discussion

Characterization of $NiFe_2O_4$

XRD analysis was utilized to characterize the crystalline phase of the as-prepared catalyst, as shown in Fig. 1a. It was clear that the catalyst exhibited several strong diffraction peaks at 30.3°, 35.7°, 43.4°, 57.5° and 63.0°, which can be indexed to the standard pattern of $NiFe_2O_4$ crystals (JCPDS: 10-0325). No common intermediate phases such as NiO and α-Fe_2O_3 were detectable, confirming its good crystallinity and pure phase. From Scherrer's equation, it could be estimated that the average size of these $NiFe_2O_4$ crystals was about 10 nm. However, these small crystals were not highly dispersed, and they assembled into bulky polyhedrons in the micron scale, as verified by SEM and TEM images (Fig. 1b and inset). An enlarged TEM image (Fig. S1) revealed that the real size of these $NiFe_2O_4$ nanoparticles was about 10~12 nm, in good agreement with XRD result. Abundant pores resulted from the interspaces among these nanoparticles can also be observed (Fig. 1b, inset), which was usually considered to favor the diffusion of reaction substrates and enhance the catalytic effectiveness. Fig. 1c showed the N_2 adsorption-desorption isotherm and pore size distribution of the as-prepared catalyst. As observed, the catalyst gave IV-type isotherm with a long and narrow hysteresis loop at relative pressure (P/P_0) from 0.4 to 1.0, and a broad pore size distribution centered at about 5~6 nm, suggesting that the porous structure herein was disordered. It was interesting that the porous structure endowed this catalyst with relatively high BET surface area, 53.5 m^2/g, as compared to those $NiFe_2O_4$ catalysts used in previous works.[19, 20] In addition, The as-prepared $NiFe_2O_4$ herein also displayed typical magnetic property with the value of saturation magnetization at 19.3 emu/g at room temperature, which made its separation from catalytic system easy (Fig. 1d).

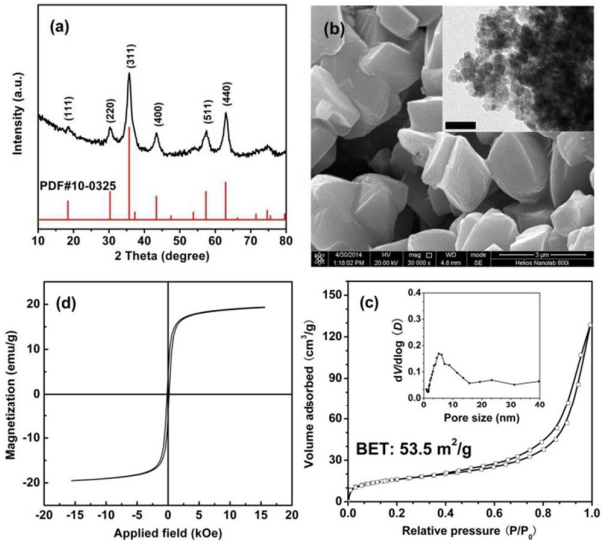

Fig. 1 XRD patterns (a), SEM and TEM (inset) images (b), N_2 isotherm and pore size distribution (inset) (c), and field-dependent curve (d) of $NiFe_2O_4$ spinel. (The scale bars for SEM and TEM are 3μm and 50 nm, respectively.)

Catalytic oxidation of benzoic acid

Fig. 2 showed BA degradation via catalytic oxidation process with different catalysts. As observed, sole PMS or $NiFe_2O_4$ failed to promise high removal efficiency of BA, suggesting that the contributions from direct PMS oxidation and $NiFe_2O_4$ adsorption were negligible. However, when both PMS (1.0 mM) and $NiFe_2O_4$ (100 mg/L) were present, over 82.5% of BA was degraded in 60 min. If $NiFe_2O_4$ was removed from the reaction system, the degradation of BA would be greatly impacted. Especially in the later stage reaction (from 30 to 60 min), the BA degradation almost kept constant, and the residual PMS and leaching nickel species (0.128 mg/L) could not afford the expected BA degradation (Fig. S2), which demonstrated the heterogeneous catalytic nature of $NiFe_2O_4$. The reference samples, NiO, Fe_2O_3 and Fe_3O_4, also exhibited their activities in the same catalytic oxidation process, especially the degradation efficiency of BA over NiO could reach 57.6%, but their performances were still much less than that of $NiFe_2O_4$. This phenomenon indicated that nickel species in heterogeneous catalysis were very eligible for PMS activation and the crystalline structure of spinel ferrites could promote their catalytic activity to a higher level. In previous reports, $NiFe_2O_4$ was rarely studied as a catalyst for heterogeneous PMS activation, thus conventional $CoFe_2O_4$ and $MnFe_2O_4$ prepared in the same way were also investigated to validate the catalytic activity of $NiFe_2O_4$. It can be found that $CoFe_2O_4$ and $MnFe_2O_4$ presented BA degradation at 86.2% and 63.8%, respectively. Although $CoFe_2O_4$ defended the best performance in BA degradation, its superiority to $NiFe_2O_4$ was rather limited. Meanwhile, ICP results revealed that $CoFe_2O_4$ produced more cobalt leaching (0.384 mg/L) as compared to nickel leaching (0.265 mg/L) and manganese leaching (0.279 mg/L) from $NiFe_2O_4$ and $MnFe_2O_4$, respectively. According to the comprehensive assessment, $NiFe_2O_4$ might be taken as a promising catalyst in SR-AOTs and deserve more concerns. In addition, the capacity of mineralization of $NiFe_2O_4$/PMS system was moderate (Fig. S3 and S4), which aligned with previous research on sulfate radicals based on homogeneous catalysis.[1] The residual organic intermediates inevitably reacted with radical species, resulting in a strong competition with BA molecules; meanwhile, the generation of radical species would gradually become slow because of the continuously decreased PMS concentration. Both of the two aspects accounted for the deceleration in degradation rate. Four recycling tests were carried out to investigate the catalytic stability of $NiFe_2O_4$ (Fig. S5). It is very interesting that the obviously decreased nickel leaching from 0.265 mg/L to 0.098 mg/L did not generate a great impact on BA degradation, and only a slight decrease in catalytic activity was presented, again verifying that heterogeneous oxidation was primary mechanism and $NiFe_2O_4$ could be an effective and stable catalyst for heterogeneous PMS activation.

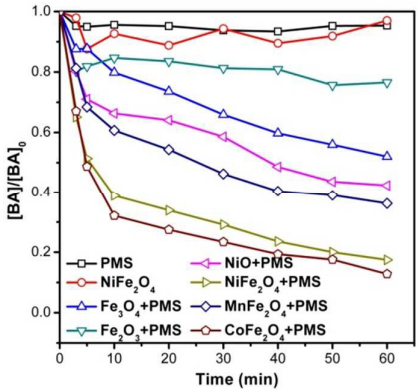

Fig. 2 BA degradation by metal oxides catalyzed PMS system. Conditions: [PMS]=1.0 mM, [BA]=10 μM, [Oxides]=100 mg/L, initial pH=7.0±0.1, T=25±1°C.

Influential factors of catalysis

Influence of initial PMS concentration and $NiFe_2O_4$ dosage

With increasing the initial PMS concentration, BA degradation was enhanced significantly (Fig. 3a). For example, the degradation efficiency of BA rose from 47.7% at 0.1mM PMS to 82.5% at 1.0 mM PMS. It is reliable that increasing PMS concentration would make more HSO_5^- attach to the active sites of $NiFe_2O_4$, which facilitated the generation of radical species. Fig. 3b showed that the degradation efficiency of BA was also improved significantly by increasing the $NiFe_2O_4$ dosage. Apparently, the increasing dosage of $NiFe_2O_4$ provided more active sites on the surface of $NiFe_2O_4$ for PMS to occupy, thus more reactive species could be generated. However, NiO as a reference gave different catalytic behaviors with increasing its dosages (Fig. S6), where BA degradation was intensified as NiO dosage was mounting from 100 mg/L to 500 mg/L, but was inefficient at higher dosages. According to previous literature,[24] this phenomenon can be related to the diffusion limitation in heterogeneous reactions. Specifically, when the dosage of NiO exceeded the optimum value, the ineffective oxidant consumption on the surface of NiO would be accelerated and become dominant before BA arriving, leading to the decreased or constant degradation efficiency. Similar phenomena had also been reported in the cases of some oxides and ferrites.[13, 14, 25, 26] In the studied interval of dosage, the diffusion limitation of $NiFe_2O_4$ was not detected, which possibly benefited from its rich porosity and relatively large BET surface that could improve the diffusion of generated radicals. This result further confirmed that $NiFe_2O_4$ herein would be a good alternative of solid catalysts for heterogeneous PMS activation.

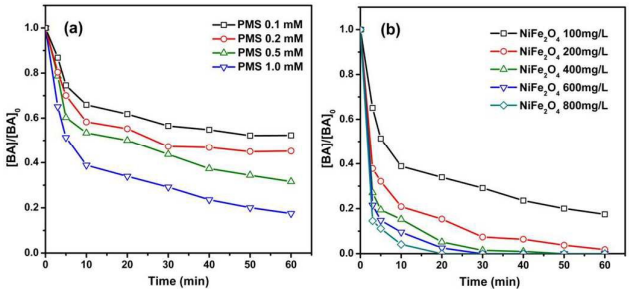

Fig. 3 Effect of PMS concentration (a) and $NiFe_2O_4$ dosage (b) on BA degradation by $NiFe_2O_4$/PMS system. Conditions: [BA]=10 μM, [$NiFe_2O_4$]=100 mg/L, initial pH=7.0±0.1, T=25±1°C.

Influence of initial pH value

The degradation efficiency of BA increased considerably as the initial pH value rose from 4.0, reached the highest value at 10.0 and decreased significantly at 11.0 (Fig. 4). Ren et al. found that the maximal decontamination efficiency was obtained around pH_{pzc} of the catalyst in the $NiFe_2O_4/O_3$ system.[19] Interestingly, the deduction was not applicable in the $NiFe_2O_4$/PMS system, since the pH_{pzc} of synthetic $NiFe_2O_4$ in this case was 7.7 and not consistent with the optimal initial pH of 10.0. To interpret the influence of initial pH, several factors should be considered, including the properties of catalyst ($NiFe_2O_4$), oxidant (PMS), organic pollutant (BA), and reactive species ($SO_4^{\cdot-}$and/or ·OH), as illustrated in Scheme 1.

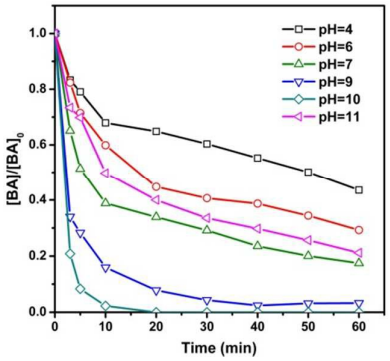

Fig. 4 Effect of initial pH value on BA degradation by $NiFe_2O_4$/PMS system. Conditions: [PMS]=1.0 mM, [BA]=10 μM, [$NiFe_2O_4$]=100 mg/L, T=25±1°C.

Firstly, the pH value determines the surface charge of $NiFe_2O_4$ through the attraction or release of protons by surface hydroxyl groups, and the surface charge of $NiFe_2O_4$ is positive at lower pH value than the pH_{pzc} and *vice versa*.[27] Secondly, pH value has a great impact on the speciation of PMS, where acidic condition induces the formation of strong H-bond between H^+ and O-O bond in PMS, and strong alkaline condition will produce less oxidative SO_5^{2-} by the deprotonation of PMS (p*Ka* of HSO_5^- is 9.4).[28] Thirdly, pH value affects the reactive species. When sulfate radicals are generated, hydroxyl radicals may also be introduced into the catalytic system, particularly under moderate alkaline condition.[29, 30] Hydroxyl radicals could not only attack organic pollutants, but also react with other species to stimulate PMS activation.[6] However, as the initial pH continuously increases, the generated $^{\cdot}OH$ (p*Ka*=11.9) becomes unstable and tends to decompose.[31] Finally, the existing form of BA is also strongly influenced by pH value in the solution, which could be converted into deprotonated $C_6H_5COO^-$ with less activity of electron donation under alkaline condition.

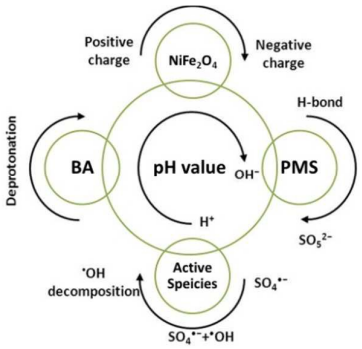

Scheme 1 Schematic illustration of the effects of pH value on the degradation system.

Considering these complexities above, the influence of initial pH value on the $NiFe_2O_4$/PMS system for BA degradation can be explained as follows. Under acidic condition, the H-bond between H^+ and PMS was dominated to inhibit the radicals generation, even though the surface charge of $NiFe_2O_4$ was attractive towards PMS. The inhibition would be weakened under neutral or alkaline condition, and HSO_5^- would be the dominating species to interact with active sites on $NiFe_2O_4$ surface. Although the deprotonated BA under alkaline condition was considered to be unfavorable for the degradation, the increasing concentration of OH^- stimulated the

generation of $^{\bullet}OH$, and more radicals guaranteed better degradation efficiency of BA. However, as the initial pH continuously increased, the decomposition of HSO_5^- (pKa=9.4) and $^{\bullet}OH$ (p*Ka*=11.9) accounted for the decline of BA degradation. Although the optimal initial pH value was 10.0, the degradation efficiency of BA under neutral condition was still considerable, which meant that $NiFe_2O_4$/PMS catalytic oxidation process was valuable and applicable within a wide pH range.

Influence of bicarbonate

Bicarbonate, which commonly exists in the natural water bodies, has been taken as radical scavengers in AOTs.[32,33] Therefore, the influence of bicarbonate should not be ignored. As shown in Fig. S7, bicarbonate displayed distinct influence at different concentration ranges, e.g. the degradation of BA was obviously enhanced at low bicarbonate concentration (≤1.0 mM), but the reverse effects were presented at high bicarbonate concentration (>1.0 mM). This phenomenon could be explained by the dual functions of bicarbonate. On one hand, bicarbonate provided buffer in the solution, which would restrain the tendency of pH decrease during the catalytic process. Considering the pH-dependence of BA degradation in $NiFe_2O_4$/PMS system, the buffer effect from bicarbonate was favorable for BA degradation. On the other hand, bicarbonate was able to scavenge radicals, resulting in the declined degradation efficiency of BA. At low concentration of bicarbonate, the buffer effect was more significant than the scavenging effect, thus the BA degradation enhanced. However, the scavenging effect would be overwhelming with increasing concentration of bicarbonate, leading to a remarkable inhibition on BA degradation.

Influence of natural organic matter

Natural organic matter (NOM) is another type of substances existing in the water, and competes with organic pollutants as radical scavenger. Some compounds of NOM (e.g. phenolic groups) might be attached on the active sites of catalyst to hinder the catalytic progress, but other compounds (e.g. quinones) may also stimulate the degradation of target organic pollutants.[34] In our case, NOM showed obvious inhibition on the degradation of BA, and the inhibition was enhanced as the initial concentration of NOM increased (Fig. S8), indicating that the detrimental effect of NOM overwhelmed the possible stimulated effect in $NiFe_2O_4$/PMS system.

Influence of halide

To testify the effectiveness of $NiFe_2O_4$/PMS for the treatment of seawater, brackish water or wastewater, KCl and KBr were added as background substance, respectively. As shown in Fig. S9a, the degradation of BA was not affected and even slightly improved when the concentration of KCl was below 0.5 mM, while the negative effect was sharply intensive as KCl concentration further increased. Compared with chloride, bromide displayed much stronger inhibition (Fig. S9b), so that there was nearly no degradation of BA when 2.0 mM KBr was present. The inhibition could be attributed to the fact that partial radicals were consumed by halides (eq 1-5), and the resultant halide radicals were less oxidative, even the kinetic rate constants from BA and halide radicals were three orders of magnitude lower than those from the reactions between BA and sulfate/hydroxyl radicals.[35] The difference in the transition process of chloride and bromide was responsible for their different inhibition. The former could be seen as a series of reversible reactions, where the forward and backward rate constants for the reaction of Cl^- with $SO_4^{\bullet-}$/$^{\bullet}OH$ are at the same magnitude,[36] thus $SO_4^{\bullet-}$/$^{\bullet}OH$ released from the backward reaction could still take part in BA degradation. For the latter, the forward rate constant for the reaction of Br^- with $SO_4^{\bullet-}$ or $^{\bullet}OH$ is much larger than the backward one (eq 6-9),[37, 38] almost resulting in complete consumption of $SO_4^{\bullet-}$/$^{\bullet}OH$.

$$^{\bullet}OH + X^- \leftrightarrow XOH^{\bullet-} \quad \text{(eq 1)}$$

$$XOH^{\bullet-} + H^+ \leftrightarrow X^{\bullet} + H_2O \quad \text{(eq 2)}$$

$$X^{\bullet} + X^- \leftrightarrow X_2^{\bullet-} \quad \text{(eq 3)}$$

$$XOH^{\bullet-} + X^- \leftrightarrow X_2^{\bullet-} + OH^- \quad \text{(eq 4)}$$

$$SO_4^{\bullet-} + X^- \leftrightarrow X^{\bullet-} + SO_4^{2-} \quad \text{(eq 5)}$$

$$^{\bullet}OH + Br^- \leftrightarrow BrOH^{\bullet-}$$

$$k_f = 1.1\times10^{10}\,M^{-1}s^{-1}, \quad k_r = 3.3\times10^{7}\,M^{-1}s^{-1} \quad \text{(eq 6)}$$

$$SO_4^{\bullet-} + Br^- \rightarrow Br^{\bullet} + 2SO_4^{2-}$$

$$k = 3.5\times10^{9}\,M^{-1}s^{-1} \quad \text{(eq 7)}$$

$$BrOH^{\bullet-} + H^+ \leftrightarrow Br^{\bullet} + H_2O$$

$$k_f = 4.4\times10^{10}\,M^{-1}s^{-1}, \quad k_r = 1.4\,M^{-1}s^{-1} \quad \text{(eq 8)}$$

$$Br^{\bullet} + Br^- \leftrightarrow Br_2^{\bullet-}$$

$$k_f = 1.0\times10^{10}\,M^{-1}s^{-1}, \quad k_r = 1.0\times10^{5}\,M^{-1}s^{-1} \quad \text{(eq 9)}$$

Influence of ion strength

Ion strength can influence the zeta potential of colloidal particles in the water. When ion strength increases, the outer-sphere interaction between particles and solute, which refers to electrostatic bonding, can be influenced, thus the decontamination efficiency will change. In contrast, covalent bonding and/or ionic bonding defined as inner-sphere complexation will rarely be affected.[39] In the $NiFe_2O_4$/PMS system, the degradation of BA was not influenced by ion strength, thus confirmed that inner-sphere interaction between HSO_5^- and active sites on $NiFe_2O_4$ surface should be the pathway of catalytic progress (Fig. S10). Also, it was verified that other phenomenon of stimulation or inhibition about BA degradation could not be attributed to the increase or decrease of ion strength.

BA degradation by $NiFe_2O_4$/PMS system in actual source water conditions

Five actual water bodies were employed to test the integrated influence of backgrounds on the degradation of BA. In I-DWTP and FW-DWTP, the degradation efficiencies of BA were 30.4% and 59.8%, respectively, which were much lower than that in Milli-Q water (Fig. 5). As discussed above, inorganic anions and natural organic matters (NOM) had obvious inhibitions on BA degradation, thus the decrease should be analyzed from two aspects. Table S1 revealed that the concentrations of total inorganic carbon (TIC) in I-DWTP and FW-DWTP were less than 12.0 mg/L (1.0 mM). Such low concentration of bicarbonate failed to produce obvious inhibition on the degradation of BA, even within the range that was positively contributed according to the aforementioned results (Fig. S7), and therefore the influence of bicarbonate was not dominant. Although the inhibition from chloride was also confirmed (Fig. S9), FW-DWTP with more chloride involved by the disinfection process still presented better degradation efficiency, being almost double as compared with that of I-DWTP, suggesting that chloride could not

be responsible for the decreased efficiencies. In contrast, the concentrations of total organic carbon (TOC) in I-DWTP and FW-DWTP were considerable (>5 mg/L), which were sufficient to deliver a blow to the degradation efficiencies (Fig. S8), not to mention the existence of some common radical scavengers, e.g. fulvic acid (Fig. S11). It was more important that the changes of degradation efficiency in I-DWTP and FW-DWTP kept in step with TOC, where the degradation efficiencies and TOC in I-DWTP and FW-DWTP were 30.4%, 11.52 mg/L and 59.8%, 5.25 mg/L, respectively, demonstrating that NOM was the primary reason for the decreased degradation efficiency.

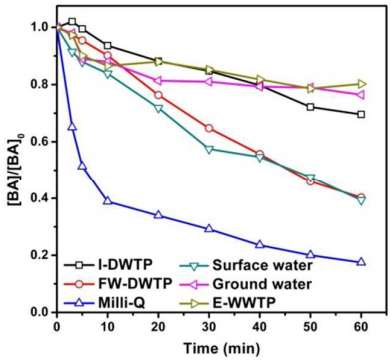

Fig. 5 BA degradation in some actual water bodies by $NiFe_2O_4$/PMS system. Conditions: [PMS]=1.0 mM, [BA]=10 μM, [$NiFe_2O_4$]=100 mg/L, initial pH=7.0±0.1, T=25±1°C.

When surface water, ground water and E-WWTP were applied as backgrounds, the degradation efficiencies of BA became 60.7%, 23.6% and 19.8%, respectively (Fig. 5). The efficiency in surface water was comparable to that in FW-DWTP (59.8%), because the components in these two water bodies were similar (Table S1). For ground water, the efficiency drastically decreased because of a large amount of bicarbonate (68.98 mg/L), which was far beyond the concentration range with positive effect (Fig. S7). With respect to E-WWTP, chloride, bicarbonate and organic compounds could be taken as the main factors that lowered the BA degradation efficiency. Besides, EEM image also revealed the presence of dissolved metabolite of microorganism in E-WWTP, which might compete with BA on radicals and result in decreased degradation efficiency (Fig. S11). Based on these results, it can be found that the degradation efficiencies of BA in FW-DWTP and surface water were acceptable due to their relative low contents of natural organic matter, bicarbonate, and chloride, which meant that $NiFe_2O_4$/PMS in AOTs could be a good choice for further advanced water treatment after conventional treatment process.

Reactive species and catalytic mechanism

Determination of reactive species

It has been verified that the contributions to BA degradation by direct PMS oxidation and $NiFe_2O_4$ adsorption were rather limited (Fig. 2), thus the radical-based oxidation process was deduced as the mechanism of BA degradation. In both homogenous and heterogeneous catalytic processes, $SO_4^{\cdot-}$ has been proved to be reactive species for decontamination.[9, 11] $^{\cdot}OH$ might be involved in the catalysis, and is always found in the heterogeneous process.[13] As typical scavengers of radical species, TBA and MeOH generally presented distinguishable difference in rate constants when they reacted with sulfate and hydroxyl radicals.[5, 31] In our case, therefore, TBA was selected as a particular scavenger for $^{\cdot}OH$, and MeOH was utilized as a universal scavenger for both $SO_4^{\cdot-}$ and $^{\cdot}OH$.

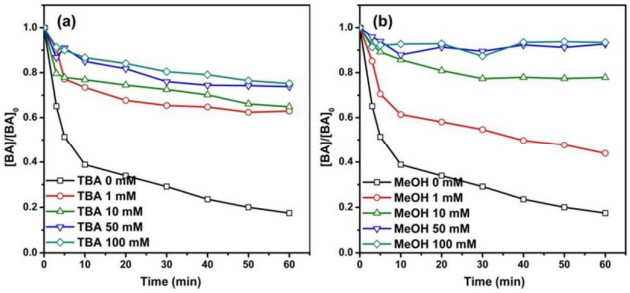

Fig. 6 Inhibition of (a) TBA and (b) MeOH on BA degradation by $NiFe_2O_4$/PMS system. Conditions: [PMS]=1.0 mM, [BA]=10 μM, [$NiFe_2O_4$]=100 mg/L, initial pH=7.0±0.1, T=25±1°C.

As shown in Fig. 6, the inhibition of TBA and MeOH on BA degradation was highly dependent on their initial concentrations. For example, the degradation efficiency of BA decreased from 82.5% to 37.1% and 50.3% in the presence of 1.0 mM of TBA and MeOH, respectively. Further increasing the concentration, MeOH began to play a more aggressive role in inhibiting BA degradation as compared with TBA, e.g. the degradation efficiencies of BA were 35.2% and 22.1% at 10 mM of TBA and MeOH, respectively. When the concentration reached 100 mM, $NiFe_2O_4$/PMS still gave the degradation efficiency of BA at 24.8% in TBA system, but it became less than 10% in MeOH system. In theory, equivalent MeOH should show stronger inhibition than TBA because MeOH could scavenge both $SO_4^{\cdot-}$ and $^{\cdot}OH$,[5, 31] however, the contrary appeared at the low concentration (0.1 mM). It was reported that hydroxylmethyl radicals ($^{\cdot}CH_2OH$) produced by the reaction of MeOH with $SO_4^{\cdot-}$/$^{\cdot}OH$ could stimulate the decomposition of PMS towards radicals and alleviate the inhibition of MeOH at low concentration.[6] Very importantly, TBA failed to inhibit the degradation efficiency of BA to a rather low level, even at very high concentration (100 mM), which was a hint that both $SO_4^{\cdot-}$ and $^{\cdot}OH$ were involved in the degradation of BA. In addition, it could be found that the inhibition of TBA at different initial pH values also changed (Fig. S12), further confirming that initial pH value was in charge of the variety and quantity of reactive species. Under acidic condition, fewer radicals were formed so that 100 mM TBA was basically sufficient for radical-scavenging. As the initial pH value increased, more radicals were generated, including $^{\cdot}OH$ from the reaction of $SO_4^{\cdot-}$ with OH^-, thus the inhibition of TBA on catalysis was weakened.

Determination of active site and possible catalytic mechanism

According to previous literature, either Fe or Ni could act as the active sites for the generation of radicals in heterogeneous AOTs.[11, 19] To discern the primary functional sites in our case, the existing state of Fe and Ni in fresh and used $NiFe_2O_4$ were characterized by XPS. As shown in Fig. S13, Fe 2p level in fresh $NiFe_2O_4$ exhibited two peaks with binding energy at 711.2 eV and 724.8 eV, which could be assigned to Fe $2p_{3/2}$ and Fe $2p_{1/2}$, respectively. After degradation, the profile of Fe 2p in used $NiFe_2O_4$ was quite similar to that of fresh $NiFe_2O_4$, and no peak shift or shoulder signal was detected, indicating that Fe sites kept their initial state during the catalytic process. In contrast, the profiles of Ni 2p in fresh and used $NiFe_2O_4$ were a little different, especially in the shake-up peaks of Ni $2p_{3/2}$. In order to better illustrate the variation, the fitting curves of Ni $2p_{3/2}$ and its shake-up peaks in fresh and used $NiFe_2O_4$ were further shown in Fig. 7a. It was clear that the component percentage of

shake-up peaks increased from 35.4% in the fresh catalyst to 53.7% in the used one. This phenomenon meant that the composition of Ni(II) and Ni(III) changed during the degradation process.[19] In general, surface complexation between metal sites and peroxo species might account for the partial transformation from Ni(II) to Ni(III).[14] However, transition metal ions with high valence, e.g. Co(III), Cu(III), Ni(III), Zn(III), were extremely active due to their high redox potential, and they could even oxidize HSO_5^- into $SO_5^{\cdot-}$ accompanied with simultaneous reduction from trivalent ions to bivalent ions.[14-16] The reversible evolution between different valences of transition metal ions was always considered to be very important for the generation of radicals,[11, 19] thus it could be concluded that Ni sites undertook the primary functions in current system.

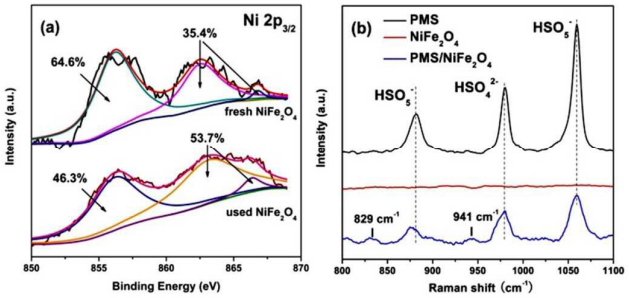

Fig. 7 XPS of Ni 2p in fresh and used $NiFe_2O_4$ (a), and Raman spectra of the PMS solution alone, $NiFe_2O_4$ particles in water, and $NiFe_2O_4$ particles in PMS solution (b).

The in situ Raman spectra revealed that there was obvious interaction between PMS and Ni sites on the surface of catalysts (Fig. 7b). On one hand, the peak corresponding to HSO_5^- displayed a slight red-shift in $NiFe_2O_4$/PMS system; on the other hand, two new small and broad peaks that could be ascribed to the formation of a peroxo species bond to surface metal sites appeared at around 829 and 941 cm^{-1}, respectively.[24, 40] These results suggested that HSO_5^- would be the first to attach to the active sites by the inner-sphere complexation during the catalytic process. This explanation was properly supported by the sharply decreased degradation efficiency of BA in the presence of phosphates (Fig. S14), where phosphates could occupy these active sites and undermine the inner-sphere complexation due to their very strong affinity to active sites.[16]

Based on the results above and previous research, the possible catalytic mechanism of radicals generation could be deduced.[41, 42] The complex, Ni(II)-$(HO)OSO_3^-$, firstly formed by the inner-sphere complexation between PMS and Ni sites on the surface of $NiFe_2O_4$, which bonded to a possible higher transient valence (eq 10). By means of one-electron transfer inside the complex, $SO_4^{\cdot-}$ were generated and new hydroxyl groups formed (eq 11). Ni(III) then oxidized PMS to $SO_5^{\cdot-}$ that further attached to the hydroxyl groups, produced the surface peroxo species, and reached a lower transient valence (eq 12). The surface peroxo species combined with each other, and recycled hydroxyl groups bonded to Ni(II) were obtained (eq 13-14). In addition, $SO_4^{\cdot-}$ that caged or bounded to the metal was found in the Ni-mediated decomposition of PMS in homogenous catalysis.[9] In this $NiFe_2O_4$/PMS system, it could be deduced that part of sulfate radicals may also be bounded on the surface of $NiFe_2O_4$, which could be consumed by catalyst or released in the solution (eq 15). Although $^{\cdot}OH$ herein contributed to BA degradation considerably, the pathway of its generation was unclear yet.[30]

$$\equiv Ni(II)\text{-}^{-}OH + HSO_5^- \rightarrow \equiv Ni(II)\text{-}(OH)OSO_3^- + OH^- \quad \text{(eq 10)}$$

$$\equiv Ni(II)\text{-}(OH)OSO_3^- \rightarrow \equiv Ni(III)\text{-}^{-}OH + SO_4^{\cdot-} \quad \text{(eq 11)}$$

$$\equiv Ni(III)\text{-}^{-}OH + HSO_5^- \rightarrow \equiv Ni(II)\text{-}^{\bullet}OOSO_3^- + H_2O \quad \text{(eq 12)}$$

$$2 \equiv Ni(II)\text{-}^{\bullet}OOSO_3^- + 2H_2O \rightarrow 2 \equiv Ni(II)\text{-}^{-}OH + O_2 + 2SO_4^{\bullet-} + 2H^+ \quad \text{(eq 13)}$$

$$2 \equiv Ni(II)\text{-}^{\bullet}OOSO_3^- + 2H_2O \rightarrow 2 \equiv Ni(II)\text{-}^{-}OH + O_2 + S_2O_8^{2-} + 2H^+ \quad \text{(eq 14)}$$

$$\equiv Ni(II)\text{-}(OH)OSO_3^-[\rightarrow \equiv Ni(III)\text{-}^{-}OH \cdots (SO_4^{\bullet-})] \rightarrow \equiv Ni(III)\text{-}^{-}OH + SO_4^{\bullet-} \quad \text{(eq 15)}$$

Conclusions

A simple and scalable method, thermal decomposition of transition metal oxalate, had been used for the preparation of $NiFe_2O_4$ with high-purity phase, large BET surface, and magnetically separable ability. The as-prepared $NiFe_2O_4$ was applied in heterogeneous catalysis to generate powerful radicals from PMS for the removal of recalcitrant pollutant. BA was chosen as a model stable organic pollutant to investigate the catalytic performance of $NiFe_2O_4$/PMS system. The excellent catalytic activity and stability demonstrated that $NiFe_2O_4$ was an effective and promising catalyst for heterogeneous PMS activation. The degradation efficiency of BA in $NiFe_2O_4$/PMS system was more or less affected by some influential factors, e.g. dosages of PMS and $NiFe_2O_4$, pH value, bicarbonate, natural organic matter, halide, ion strength. BA degradation by $NiFe_2O_4$/PMS system was also carried out under different actual water background conditions, where the surface water and the finished water from drinking water treatment plants kept the degradation efficiencies of BA in an acceptable level (*ca.* 60%) due to their low contents of natural organic matter, bicarbonate, and chloride. This implied that $NiFe_2O_4$/PMS system should better be placed after conventional treatment process for further advanced water treatment. By capturing radical species with TBA and MeOH, sulfate radicals and hydroxyl radicals were confirmed to be the main reactive species. The results of XPS and Raman spectra revealed that Ni sites on the surface were primarily active sites, and their interaction with HSO_5^- through inner-sphere complexation was responsible for the efficient generation of radicals.

Acknowledgements

This work is supported by Open Project of State Key Laboratory of Urban Water Resource and Environment, HIT (QA201414), China Postdoctoral Science Foundation (2013M541394 and 2014T70341), the National Science & Technology Pillar Program, China (2012BAC05B02), National Natural Science Foundation of China (51378141 and 51008104), and Fundamental Research Funds for the Central Universities and Program for Innovation Research of Science in HIT (B201411).

Notes and references

1 G. P. Anipsitakis and D. D. Dionysiou, *Environ. Sci. Technol.*, 2003, **37**, 4790-4797.

2 S. Esplugas, J. Giménez, S. Contreras, E. Pascual and M. Rodrìguez, *Water Res.*, 2002, **36**, 1034-1042.
3 Y. P. Zhu, T. Z. Ren and Z. Y. Yuan, *RSC Adv.*, 2015, **5**, 7628-7636.
4 G. P. Anipsitakis and D. D. Dionysiou, *Appl. Catal. B-Environ.*, 2004, **54**, 155-163.
5 P. Neta, R. E. Huie and A. B. Ross, *J. Phys. Chem. Ref. Data*, 1988, **17**, 1027-1284.
6 Y. H. Guan, J. Ma, X. C. Li, J. Y. Fang and L. W. Chen, *Environ. Sci. Technol.*, 2011, **45**, 9308-9314.
7 L. Hou, H. Zhang and X. Xue, *Sep. Purif. Technol.*, 2012, **84**, 147-152.
8 S. Yang, P. Wang, X. Yang, L. Shan, W. Zhang, X. Shao and R. Niu, *J. Hazard. Mater.*, 2010, **179**, 552-558.
9 G. P. Anipsitakis and D. D. Dionysiou, *Environ. Sci. Technol.*, 2004, **38**, 3705-3712.
10 P. R. Shukla, S. B. Wang, H. Q. Sun, H. M. Ang and M. Tade, *Appl. Catal. B-Environ.*, 2010, **100**, 529-534.
11 Y. Ding, L. Zhu, N. Wang and H. Tang, *Appl. Catal. B-Environ.*, 2013, **129**, 153-162.
12 J. Deng, Y. Shao, N. Gao, C. Tan, S. Zhou and X. Hu, *J. Hazard. Mater.*, 2013, **262**, 836-844.
13 Y. H. Guan, J. Ma, Y. M. Ren, Y. L. Liu, J. Y. Xiao, L. Q. Lin and C. Zhang, *Water Res.*, 2013, **47**, 5431-5438.
14 T. Zhang, H. Zhu, J. P. Croué, *Environ. Sci. Technol.*, 2013, **47**, 2784-2791.
15 Y. Yao, Y. Cai, F. Lu, F. Wei, X. Wang and S. Wang, *J. Hazard. Mater.*, 2014, **270**, 61-70.
16 Y. Ren, L. Lin, J. Ma, J. Yang, J. Feng and Z. Fan, *Appl. Catal. B-Environ.*, 2015, **165**, 572-578.
17 Y. X. Wang, H. Q. Sun, H. M. Ang, M. O. Tade and S. B. Wang, *ACS Appl. Mater. Interfaces*, 2014, **6**, 19914-19923.
18 B. Yang, Z. Tian, B. Wang, Z. B. Sun, L. Zhang, Y. P. Guo, H. Z. Li and S. Q. Yan, *RSC Adv.*, 2015, **5**, 20674-20683.
19 Y. Ren, Q. Dong, J. Feng, J. Ma, Q. Wen and M. Zhang, *J. Colloid Interf. Sci.*, 2012, **382**, 90-96.
20 H. Zhao, Y. Dong, G. Wang, P. Jiang, J. Zhang, L. Wu and K. Li, *Chem. Eng. J.*, 2013, **219**, 295-302.
21 A. A. Ajmera, S. B. Sawant, V. G. Pangarkar and A. A. C. M. Beenackers, *Chem. Eng. Technol.*, 2002, **25**, 173-180.
22 L. Guo, H. Arafune and N. Teramae, *Langmuir*, 2013, **29**, 4404-4412.
23 J. A. Menéndez, J. Phillips, B. Xia and L. R. Radovic, *Langmuir*, 1996, **12**, 4404-4410.
24 W. Najjar, S. Azabou, S. Sayadi and A. Ghorbel, *Appl. Catal. B-Environ.*, 2007, **74**, 11-18.
25 H. Liang, H. Sun, A. Patel, P. Shukla, Z. H. Zhu and S. B. Wang, *Appl. Catal. B-Environ.*, 2012, **127**, 330-335.
26 L. Hou, H. Zhang, L. Wang, L. Chen, Chem. Eng. J., 2013, 229, 577-584.
27 J. Ma, M. Sui, T. Zhang and C. Guan, *Water Res.*, 2005, **39**, 779-786.
28 S. K. Rani, D. Easwaramoorthy, I. M. Bilal and M. Palanichamy, *Appl. Catal. A-Gen.*, 2009, **369**, 1-7.
29 S. Yuan, P. Liao and A. N. Alshawabkeh, *Environ. Sci. Technol.*, 2014, **48**, 656-663.
30 J. Zou, J. Ma and J. Zhang, *Environ. Sci. Technol.*, 2014, **48**, 4630-4631.
31 G. V. Buxton, C. L. Greenstock, W. P. Helman and A. B. Ross, *J. Phys. Chem. Ref. Data*, 1988, **17**, 513-886.
32 J. De Laat, Y. H. Dao, N. Hamdi El Najjar and C. Daou, *Water Res.*, 2011, **45**, 5654-5664.
33 V. Shafirovich, A. R. Dourandin, W. Huang and N. E. Geacintov, *J. Biol. Chem.*, 2001, **276**, 24621-24626.
34 G. Fang, J. Gao, D. D. Dionysiou, C. Liu and D. Zhou, *Environ. Sci. Technol.*, 2013, **47**, 4605-4611.
35 Y. Yang, J. J. Pignatello, J. Ma and W. A. Mitch, *Environ. Sci. Technol.*, 2014, **48**, 2344-2351.
36 G. V. Buxton, M. Bydder and G. Salmon, *Phys. Chem. Chem. Phys.*, 1999, **1**, 269-273.
37 H. V. Lutze, R. Bakkour, N. Kerlin, C. von Sonntag and T. C. Schmidt, *Water Res.*, 2014, **53**, 370-377.
38 J. E. Grebel, J. J. Pignatello and W. A. Mitch, *Environ. Sci. Technol.*, 2010, **44**, 6822-6828.
39 W. Stumm, *Chemistry of the solid-water interface: Processes at the mineral-water and particle-water interface in natural systems*, John Wiley & Son Inc., New York, 1992.
40 T. Zhang, W. Li and J. P. Croué, *Environ. Sci. Technol.*, 2011, **45**, 9339-9346.
41 T. Zhang, Y. Chen, Y. Wang, J. Le Roux, Y. Yang and J. P. Croué, *Environ. Sci. Technol.*, 2014, **48**, 5868-5875.
42 L. Q. Hatcher and K. D. Karlin, *J. Biol. Inorg. Chem.*, 2004, **9**, 669-683.

Graphical Abstract

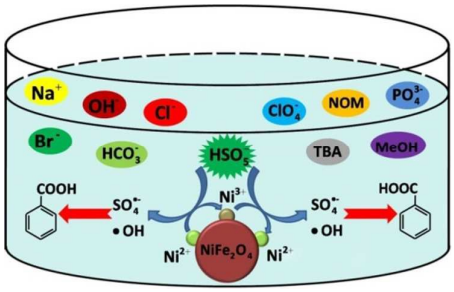

Catalytic performance of $NiFe_2O_4$/PMS system as advanced oxidation technologies in pure water and actual water was studied, and various influential factors and catalytic mechanism were also investigated.